

Effect of grain size on the transition between ferroelectric and relaxor states in $0.8\text{Pb}(\text{Mg}_{1/3}\text{Nb}_{2/3})\text{O}_3\text{-}0.2\text{PbTiO}_3$ ceramics

R. Jiménez,¹ H. Amorín,¹ J. Ricote,¹ J. Carreaud,² J. M. Kiat,^{2,3} B. Dkhil,² J. Holc,⁴ M. Kosec,⁴ and M. Algueró¹

¹*Instituto de Ciencia de Materiales de Madrid, CSIC, Cantoblanco, 28049 Madrid, Spain*

²*Laboratoire Structures, Propriétés et Modélisation des Solides, UMR8580-CNRS, Ecole Centrale Paris, Grande Voie des Vignes, 92295 Châtenay-Malabry, France*

³*Laboratoire Léon Brillouin, CE Saclay, 91191 Gif-sur-Yvette Cedex, France*

⁴*Institute Jozef Stefan, Jamova 39, 1000 Ljubljana, Slovenia*

(Received 29 May 2008; published 4 September 2008)

The phase transition between the ferroelectric and relaxor states in $0.8\text{Pb}(\text{Mg}_{1/3}\text{Nb}_{2/3})\text{O}_3\text{-}0.2\text{PbTiO}_3$ ceramics with decreasing grain sizes in the submicron range, down to the nanoscale, has been studied with measurements of the temperature dependence of the dielectric and elastic properties across the transition. Results indicate that main size effects are the shift of the transition toward lower temperatures when grain size decreases and the sharp slowing down of its kinetics below a size of $0.36\ \mu\text{m}$. This is consistent with the existence of a well defined temperature of slowing down of the transition in the temperature interval between 334 and 338 K for $0.8\text{Pb}(\text{Mg}_{1/3}\text{Nb}_{2/3})\text{O}_3\text{-}0.2\text{PbTiO}_3$. Rietveld analysis of x-ray diffraction patterns indicates that kinetics mainly control the scale of the Cm monoclinic distortions within an average $R3m$ rhombohedral phase, which decreases with grain size, analogously to the effect of decreasing the amount of PbTiO_3 in the solid solution. The scale of the monoclinic order strongly affects ferroelectric switching, which is hindered when it is short ranged.

DOI: [10.1103/PhysRevB.78.094103](https://doi.org/10.1103/PhysRevB.78.094103)

PACS number(s): 77.84.Dy, 68.35.Rh, 68.60.Bs

I. INTRODUCTION

Ferroelectric perovskite, morphotropic phase boundary (MPB) $\text{Pb}(\text{Zr},\text{Ti})\text{O}_3$ (PZT)-based ceramics are the active elements in a wide range of piezoelectric devices such as sensors and actuators, ultrasound technologies, and underwater acoustics.¹ Their high electromechanical activity is associated with the presence of a monoclinic phase between the rhombohedral and tetragonal phases in the MPB region² and a mechanism of polarization rotation among the phases.^{3,4} The most sensitive commercial PZT-based materials are the soft PZT ceramics, for which d_{33} piezoelectric coefficients up to $\sim 600\ \text{pC N}^{-1}$ are obtained by additional composition engineering of the Curie temperature and domain-wall mobility.⁵ MPBs can be found in other systems such as the $\text{Pb}(\text{Zn}_{1/3}\text{Nb}_{2/3})\text{O}_3\text{-PbTiO}_3$ (PZN-PT), $\text{Pb}(\text{Mg}_{1/3}\text{Nb}_{2/3})\text{O}_3\text{-PbTiO}_3$ (PMN-PT), and $\text{Pb}(\text{Sc}_{1/2}\text{Nb}_{1/2})\text{O}_3\text{-PbTiO}_3$ (PSN-PT) relaxor-ferroelectric solid solutions.⁶⁻⁸ These systems are being considered as an alternative to PZT-based materials, for single crystals, and textured ceramics present piezoelectric coefficients above $1500\ \text{pC N}^{-1}$ by the mechanism of polarization rotation.^{9,10} Piezoelectric devices are not oblivious to the current miniaturization trends in ceramic technology for microelectronics. Multilayer ceramic capacitors (MLCC) are being scaled down,¹¹ and an analogous trend can be anticipated for multilayer ceramic actuators (MLCA) and for other piezoelectric device configurations.¹² With the ceramic layers approaching thickness of $1\ \mu\text{m}$, grain size must be decreased down to the submicron range close to the nanoscale ($\rightarrow 100\ \text{nm}$) because at least 5–10 grains per layer are necessary for the element reliability. The size reduction is even more important for thinner piezoelectric layers integrated in microelectromechanical systems.¹³ This raises the question

on how properties are affected by the size reduction.

Most of the studies on size effects in polycrystals have focused on tetragonal BaTiO_3 as the active element of MLCC. The room-temperature (RT) dielectric permittivity and ferroelectric hysteresis loops of BaTiO_3 ceramics present a distinctive variation with grain size¹⁴⁻¹⁶ that is associated with the evolution of the ferroelectric domain configuration, basically with the density of 90° walls¹⁷ and their dynamics;¹⁸ the stress caused by the ceramic clamping reduces the domain-wall mobility as the size is reduced. This stress reaches its highest level with the disappearance of the 90° domains below a certain grain size, which is $\sim 0.3\ \mu\text{m}$ for BaTiO_3 .¹⁴ Nonlinear thermodynamic theory shows that the clamping modifies the room-temperature phase of the single domain crystals, so as coexistence of rhombohedral and orthorhombic phases is present, instead of the tetragonal phase.¹⁹ New phenomena might appear with further decrease of size. Ferroelectricity is a cooperative phenomenon, and it was long thought that a minimum volume was necessary to sustain the polar state. This raises the existence of a fundamental size limit below which ferroelectricity vanishes,^{20,21} which would set a lower limit for the downscaling of piezoelectric ceramic devices. In the case of BaTiO_3 , dense ceramics with a grain size of $20\ \text{nm}$ still present the anomaly in the temperature dependence of the dielectric permittivity associated with the transition between the ferroelectric and paraelectric states. However, ferroelectric switching was not observed in the nanostructured material.²²

Less attention has been paid to size effects on the electromechanical properties of MPB materials. The d_{33} piezoelectric coefficient of soft PZT ceramics continuously decreases with grain size from $550\ \text{pC N}^{-1}$ for $4\ \mu\text{m}$, down to $350\ \text{pC N}^{-1}$ for $0.17\ \mu\text{m}$, attributed to the decrease of the ferroelectric/ferroelastic domain-wall mobility because of ce-

TABLE I. Average grain size and standard deviation (SD) of the 0.8PMN-0.2PT ceramic samples processed by hot pressing of the nanocrystalline powder at decreasing temperatures (after Ref. 34). Symmetry and cell parameters of the room-temperature phases are also given (after Ref. 27).

	Average grain size	SD	Symmetry	Cell parameters
1273 K	0.36 μm	0.12 μm	<i>Cm</i>	$a=5.6982 \text{ \AA}$, $b=5.6953 \text{ \AA}$, $c=4.0289 \text{ \AA}$, $\beta=89.94^\circ$
1173 K	0.21 μm	0.07 μm	<i>Cm</i>	$a=5.6989 \text{ \AA}$, $b=5.6955 \text{ \AA}$, $c=4.0295 \text{ \AA}$, $\beta=89.99^\circ$
1073 K	0.14 μm	0.05 μm	<i>R3m</i>	$a=4.0300 \text{ \AA}$, $\beta=89.99^\circ$
973 K	90 nm	30 nm	<i>R3m</i>	$a=4.0300 \text{ \AA}$, $\beta=89.99^\circ$

ramic clamping.²³ The nonlinear thermodynamic theory also predicts a modification of the room-temperature phases of single domain PZT crystals by the clamping.¹⁹ In relation to the size limit of ferroelectricity, ferroelectric switching has been observed in a thin-film coating of PZT particles with a size of 9 nm.²⁴ Recently, relaxor-based materials have started to be investigated. The size effect has been studied for 0.65PMN-0.35PT at the core of the MPB region; structural characterization and results on dielectric properties of bulk compacts indicated that the high-temperature relaxor state was still present at room temperature for sizes below 0.2 μm instead of the ferroelectric phase.²⁵ RT relaxor-type electrical behavior has been also reported for 0.92PZN-0.02PT nanostructured materials with a grain size of 20 nm.²⁶ Back to PMN-PT, we have studied the RT phases in ceramics of 0.8PMN-0.2PT at the PMN edge of the MPB region with decreasing size down to the nanoscale (<100 nm) and found a size-driven transition from a monoclinic to a rhombohedral phase between 0.25 and 0.15 μm .²⁷

We report here the size effect on the transition between the relaxor and ferroelectric states of 0.8PMN-0.2PT. Main features of the transition have recently been established for coarse-grained ceramics of this composition by studying the temperature dependence of the dielectric permittivity and the Young's modulus across the transition, in combination with ferroelectric hysteresis loops and structural characterization.²⁸ 0.8PMN-0.2PT shows a transition between the monoclinic *Cm* ferroelectric phase and the nonergodic relaxor state with well defined, separated transition ($T_{Ch}=344 \text{ K}$ and $T_{Cc}=334 \text{ K}$ on heating and cooling, respectively) and freezing ($T_f=350 \text{ K}$) temperatures. The transition also presents thermal hysteresis in the kinetics that is much slower on cooling than on heating. This slowing down was discussed within the frame of the two-stage model for the development of ferroelectric long-range order in relaxor systems proposed by Bokov²⁹ and Ye *et al.*³⁰ We have used the same methodology on a series of 0.8PMN-0.2PT ceramic samples with decreasing grain size down to the nanoscale to study the size effect on the transition between the relaxor and ferroelectric states. Results indicate that the size effects on the actual room-temperature phase and its ferroelectric properties are a consequence of a size effect on the ferroelectric phase transition, especially on its kinetics, and provide further support to the existence of a well defined temperature of slowing down of the transition in the relaxor-based system.

II. EXPERIMENT

0.8PMN-0.2PT ceramic samples with submicron grain sizes down to less than 100 nm were processed by hot pressing of nanocrystalline powder. This powder was obtained by mechanochemical activation of the binary oxides without any excess of PbO and MgO, which has been considered essential for properly controlling composition when addressing fundamental studies in the PMN-PT system.³¹ A high energy planetary mill and tungsten carbide milling media were used. Contamination from the WC:Co milling media was controlled below 50 and 600 ppm of Co and W, respectively. Details of the procedures and of the mechanisms taking place during the activation can be found elsewhere.³² The powder allows the processing of coarse-grained ceramics with high chemical homogeneity and crystallographic quality by sintering in a PbO rich atmosphere³³ and obtaining submicron grain sizes by hot pressing.³⁴ Ceramic samples here studied were hot pressed at 60 MPa and 1273, 1173, 1073, and 973 K. Dense (>90%) single phase materials were obtained for all temperatures, except for the ceramic processed at 973 K, which presented traces of residual pyrochlore phase. Grain-size distributions were measured by quantitative image analysis of scanning force microscopy data. Single lognormal distributions were found for all cases, whose averages and standard deviations are given in Table I. Note that the average size ranged between 0.36 μm and 90 nm. More details can be found in Ref. 35. Previously reported symmetry and cell parameters of the room-temperature phases as determined by Rietved analysis of XRD data are also given in the table.²⁷

Electrical characterization was carried out on ceramic disks on which Ag electrodes had been painted and sintered at 923 K. The dependence of the dielectric permittivity and losses on temperature were measured with a HP 4284A precision LCR meter at 0.1, 1, 10, 100, and 1000 kHz. Measurements were dynamically accomplished at $\pm 1.5 \text{ K min}^{-1}$ during a heating/cooling cycle: from 77 to 523 K and back below room temperature. Room-temperature ferroelectric hysteresis loops were obtained by current integration. Voltage sine waves of 0.1 Hz frequency and amplitudes up to 1000 V were applied by the combination of a synthesizer/function generator (HP 3325B) and a bipolar operational power supply/amplifier (KEPCO BOP 1000M). Both the charge to voltage converter and the software for loop acqui-

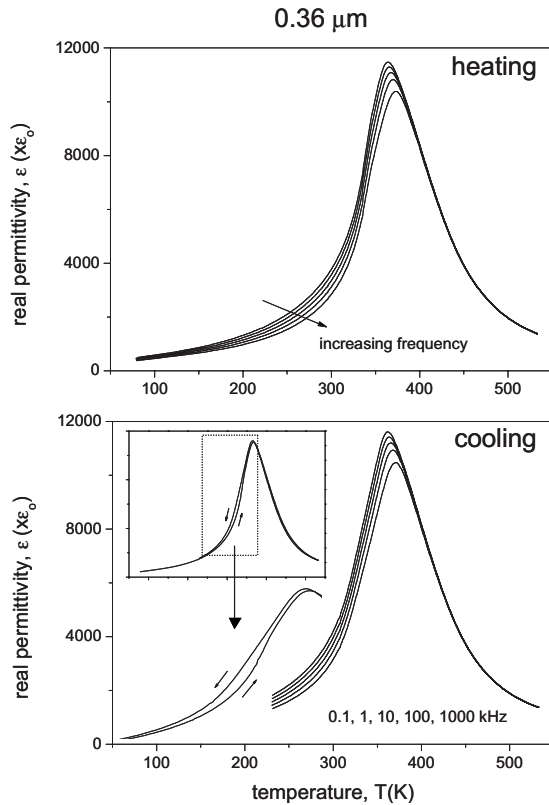


FIG. 1. Dielectric permittivity as a function of temperature at five frequencies measured during successive heating and cooling for a 0.8PMN-0.2PT ceramic with an average grain size of $0.36 \mu\text{m}$. The inset shows the permittivity at 10 kHz along the heating/cooling cycle.

sition and analysis were home built. Loops were also measured as a function of temperature on heating from 77 K to RT.

The low-frequency Young's modulus and mechanical losses were measured as a function of temperature by dynamical mechanical analysis in the three-point bending configuration with a Perkin Elmer DMA7 apparatus. A stress sine wave of 8.5 MPa amplitude, superimposed on a static stress of 10 MPa, was applied to ceramic bars of $12 \times 2 \times 0.35 \text{ mm}^3$ dimensions. Measurements were dynamically accomplished at a single frequency of 9 Hz during a cooling/heating cycle: from 523 to 77 K and back to high temperature with $\pm 2 \text{ K min}^{-1}$ rates. This technique has been shown to be very suitable for studying phase transitions^{36,37} and the dynamics of domain walls in ferroelectrics.³⁸

III. RESULTS

Results of dielectric permittivity as a function of temperature for the material with an average grain size of $0.36 \mu\text{m}$ are shown in Fig. 1. On heating, the permittivity increased with an increasing derivative until $\sim 340 \text{ K}$, at which the derivative sharply decreased. Non-negligible dispersion that also increased with temperature was observed in this range. At higher temperature, relaxor-type behavior was found, dispersion further raised, and the permittivity presented a broad

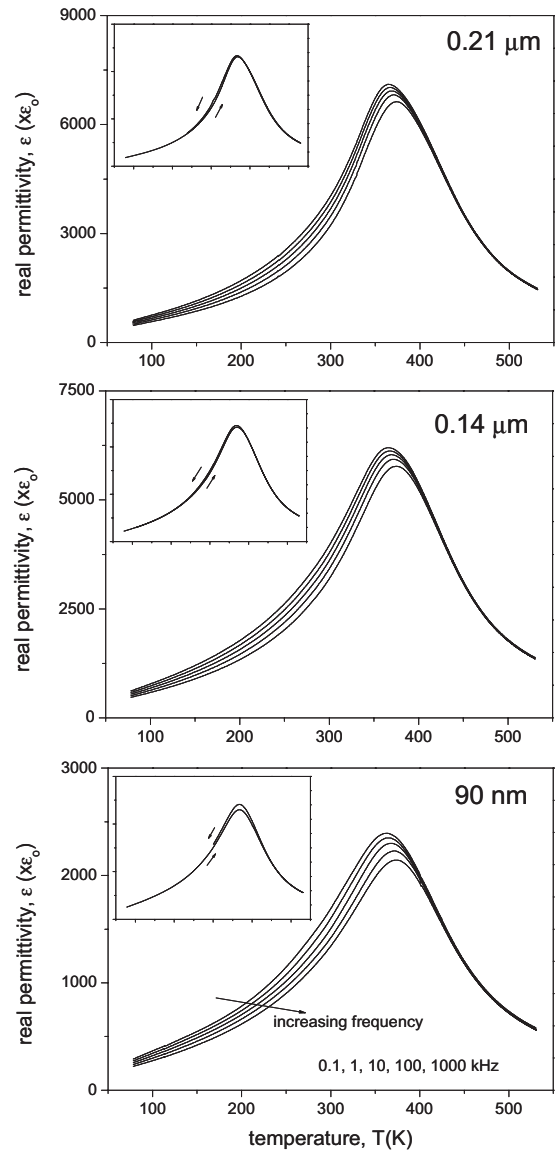


FIG. 2. Dielectric permittivity as a function of temperature at five frequencies measured during heating for 0.8PMN-0.2PT ceramics with decreasing grain sizes down to the nanoscale. The insets show the permittivity at 10 kHz along a heating/cooling cycle.

maximum that shifted toward higher temperature with frequency, from 364 K at 100 Hz to 373 K at 1 MHz. In contrast, permittivity measured on cooling presented a relaxor behavior down to 230 K, and a sharp increase in the derivative was not observed at any temperature. The thermal hysteresis is better illustrated in the inset of Fig. 1 that shows the permittivity at 10 kHz along the heating/cooling cycle; the hysteresis is evident in the 250–340 K interval.

Analogous results for the materials with an average grain size of $0.21 \mu\text{m}$, $0.14 \mu\text{m}$, and 90 nm are shown in Fig. 2. Sharp changes of the derivative were not observed on heating nor on cooling, and the thermal hysteresis was negligible. Note that dispersion vanishes at high temperature above the maxima in permittivity for all samples as expected for relaxors, which indicates the absence of Maxwell-Wagner type polarization at the grain boundaries that is usually associated

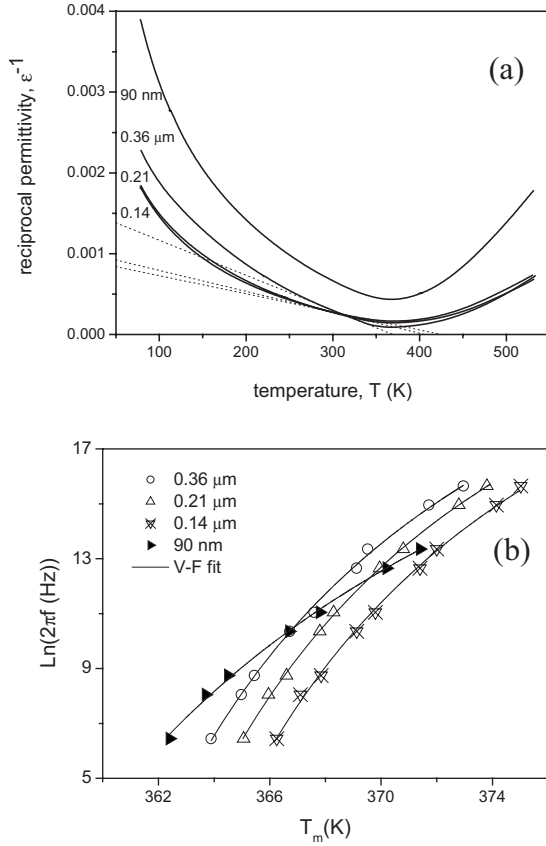


FIG. 3. (a) Temperature dependence of the reciprocal permittivity at 10 kHz measured during heating and (b) dependence of the temperature of the maximum dielectric permittivity on frequency and fit to a Vogel-Fulcher relationship, for the 0.8PMN-0.2PT ceramics with decreasing grain size down to the nanoscale.

with the presence of segregated second phases or defects.³⁹ The reciprocal permittivity at 10 kHz as a function of temperature is shown in Fig. 3(a) for the four materials. Data on heating are given, yet analogous results were obtained on cooling. Note that very similar permittivity values were found at high temperature above the maxima for the materials with a grain size of 0.36, 0.21, and 0.14 μm , which further supports the quality of the boundaries. The lower permittivity for the nanostructured material could be partially caused by the traces of residual pyrochlore phase. A Curie-Weiss behavior was not found above the temperature of the maximum permittivity as expected for a relaxor. On the contrary, the reciprocal permittivity did present a linear behavior below this temperature, down to 260–280 K, for the materials with a size of 0.36, 0.21, and 0.14 μm , which indicates the presence of a ferroelectric phase,²⁸ in good agreement with Rietveld results (see Table I). Below 260 K, a new deviation of linearity was observed. The temperature interval of the linear behavior decreased with size, so as such a regime was not found for the nanometer scale material.

The dependence on frequency of the temperature of the maximum dielectric permittivity along with the fit to a Vogel-Fulcher relationship is shown in Fig. 3(b) for all materials. The freezing temperature T_f and activation energy E_a obtained from the fit are given in Table II. A trend with size

TABLE II. Parameters of the Vogel-Fulcher behavior for the high-temperature relaxor state (T_f , E_a) and transition temperatures from mechanical properties (T_{C^c} , T_{C^h}) of 0.8PMN-0.2PT ceramic samples as a function of the average grain size.

g	T_f (K)	E_a (meV)	T_{C^c} (K)	T_{C^h} (K)
0.36 μm	350 ± 1	30 ± 2	328	338
0.21 μm	351 ± 1	29 ± 2	327	332
0.14 μm	352 ± 1	30 ± 2	299	304
90 nm	340 ± 2	47 ± 2	-	-

is not found down to 0.14 μm , and values of ~ 351 K and ~ 30 meV are obtained. However, T_f decreases down to 340 K for the nanostructured material, while E_a increases up to 47 meV.

Results of the Young’s modulus for the material with an average grain size of 0.36 μm are shown in Fig. 4. Young’s modulus Y decreased with temperature on cooling until 328 K, at which a broad and asymmetric minimum is observed. Below this temperature the Young’s modulus continuously increased down to 77 K. On subsequent, immediate heating, Y decreased until 338 K, at which it presented a minimum much sharper than that observed on cooling, and then increased up to 523 K. An inflection point was observed at 350 K at which the derivative sharply decreased. The minima are associated with the transition between the ferroelectric and relaxor states, and provide thus the transition temperatures on cooling and heating. Differences in sharpness are consistent with the thermal hysteresis in permittivity, and indicate

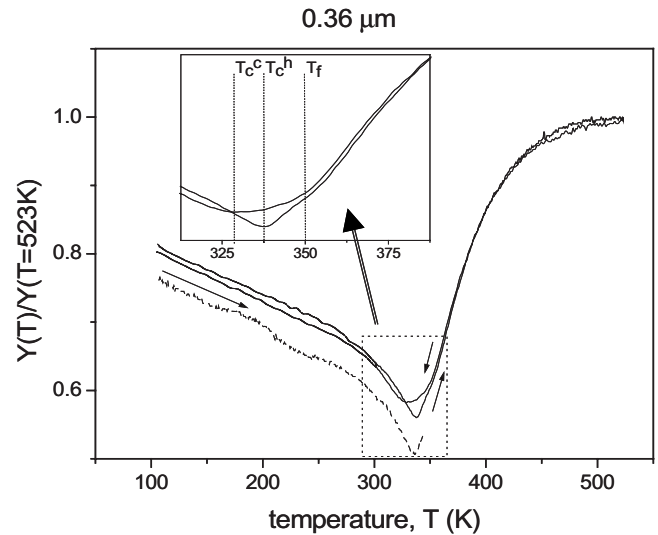


FIG. 4. Normalized (to its value at 523 K) Young’s modulus Y as a function of temperature measured during successive cooling and immediate heating for a 0.8PMN-0.2PT ceramic with an average grain size of 0.36 μm (solid lines). The inset shows a detail of the temperature interval where the phase transition takes place. The transition temperatures T_{C^c} and T_{C^h} and the freezing temperature of the high-temperature relaxor state T_f are indicated. Y measured on heating after having maintained the sample at 77 K for 1 h is also shown (dashed line).

differences in the kinetics of the transition; the slower it is the broader the minimum.²⁸ The inflection point above the transition temperature on heating takes place at the freezing temperature of the relaxor state when the polar nanoregions (PNRs) start contributing to the mechanical response.⁴⁰ The behavior of the Young's modulus on heating from 77 K presents a new feature at 200–250 K when the sample was maintained at 77 K for some time after cooling.

Analogous results for the materials with an average grain size of 0.21 μm , 0.14 μm , and 90 nm are shown in Fig. 5. Broad minima were observed on cooling and heating associated with the relaxor-ferroelectric transition with no significant differences in broadness. Transition temperatures are given in Table II; a shift toward lower temperatures when grain size decreases is evident. Data on heating shown in the figure correspond to the case for which the sample was maintained at 77 K for 1 h between cooling and heating, and the elastic anomaly at 200–250 K was observed for all sizes down to 90 nm. The actual transition temperatures for the nanostructured ceramic cannot be determined because of the broadness of the minima and some overlapping with the low-temperature anomaly on heating, but it seems fairly consistent with the trend described above with decreasing size.

Mechanical losses measured on heating after maintaining the samples at 77 K for 1 h are shown in Fig. 6 for the ceramics with a grain size of 0.36, 0.21, and 0.14 μm . Noise in the measurement of the phase shift between displacement and force was very high for the ceramic with 90 nm, and results are not shown. Two peaks were observed for the three samples: a first one at ~ 235 K and a second one at higher temperature, whose position shifts down when size decreases—from 337 K for 0.36 μm to 331 and 310 K for 0.21 and 0.14 μm . This second peak is associated with the minimum of the Young's modulus and thus with the ferroelectric to relaxor transition. The first peak at ~ 235 K takes places at the temperature at which the new anomaly in Y was observed and its height increases as size decreases. This peak seems to be somehow coupled with that of the ferroelectric to relaxor phase transition in the sense that an increase in its height results in a decrease in the height of the transition peak. However, one has to be cautious when comparing values of losses among different samples because, unlike relative sensitivity that is below 1%, the absolute sensitivity of the technique is not better than 20%.⁴¹ This is why dynamic mechanical analysis is better suited to study variations of the mechanical coefficients with a parameter, for instance temperature, than for the determination of absolute values. The coupling between the two peaks is demonstrated when comparing the mechanical losses measured on heating and cooling on the samples, which is also done in Fig. 6 for the ceramic with a grain size of 0.21 μm . This also demonstrates that the physical phenomenon responsible for the Young's modulus anomaly and mechanical loss peak at ~ 235 K also occurs on cooling, yet is hardly reflected by Y .

Finally, room-temperature ferroelectric hysteresis loops for these ceramics are shown in Fig. 7. The loop for a 0.8PMN-0.2PT ceramic with a grain size of 4 μm , processed from the same powder obtained by mechanosynthesis, is included for comparison. The ceramic with a grain size of 0.36 μm presented saturation P_s and remnant P_r polariza-

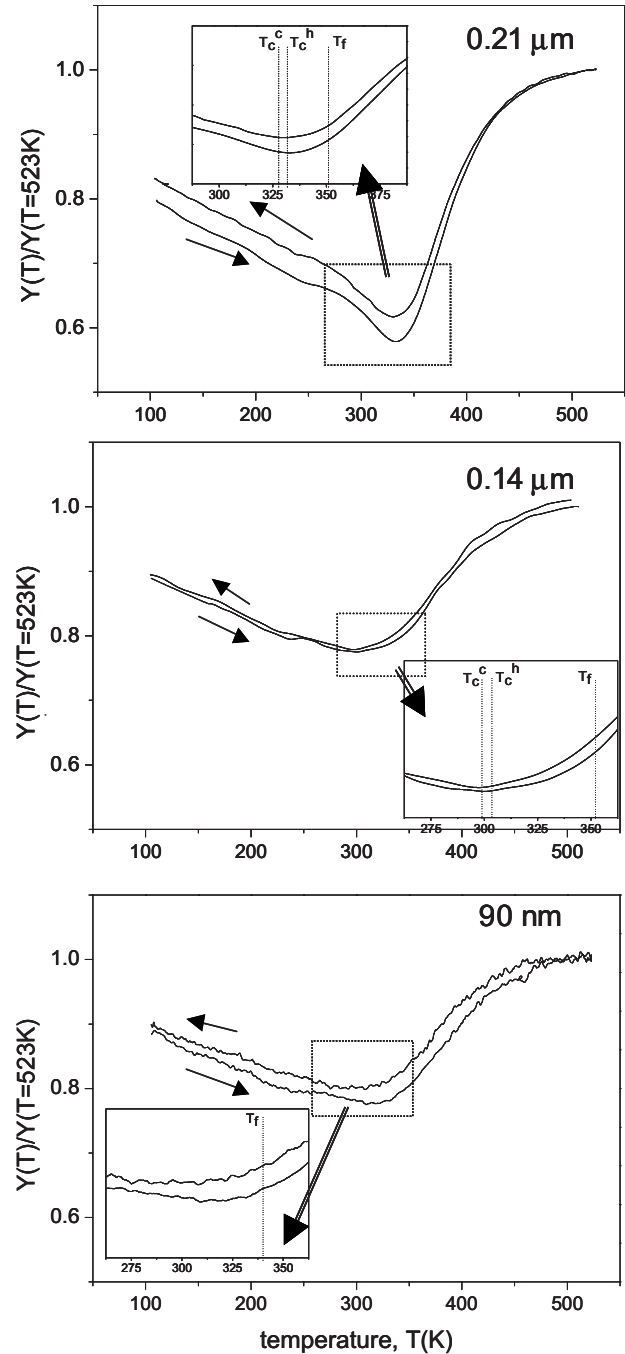


FIG. 5. Normalized (to its value at 523 K) Young's modulus Y as a function of temperature measured during successive cooling and heating, after having maintained the sample at 77 K for 1 h, for 0.8PMN-0.2PT ceramics with decreasing grain sizes down to the nanoscale. The inset shows a detail of the temperature interval where the phase transition takes place. The transition temperatures T_{C^c} and T_{C^h} and the freezing temperature of the high-temperature relaxor state T_f are indicated.

tions of 23 and 11 $\mu\text{C cm}^{-2}$, which must be compared with 25 and 21 $\mu\text{C cm}^{-2}$ for the coarse-grained material. These parameters dropped down to 14 and 7 $\mu\text{C cm}^{-2}$ for the ceramic with 0.21 μm , and only incipient switching was observed for those with 0.14 μm and 90 nm at 2 kV mm^{-1} . Loops as a function of temperature for the ceramic with a

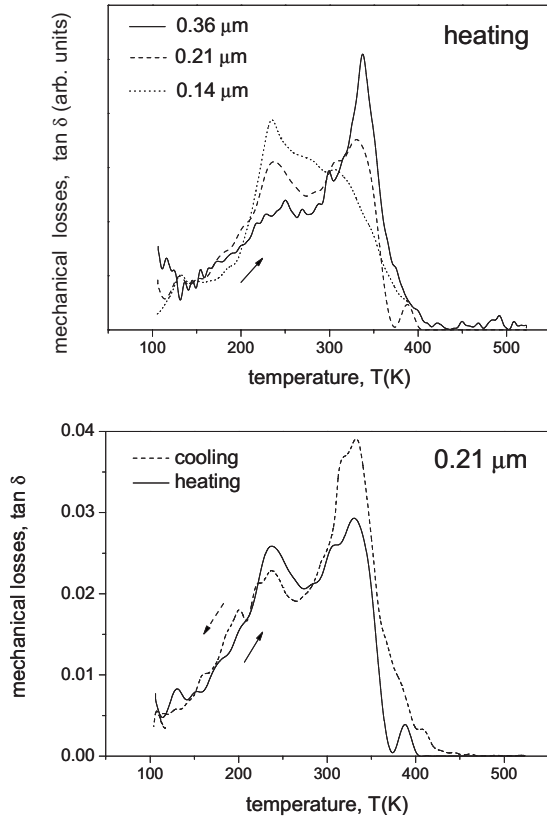


FIG. 6. Mechanical losses as a function of temperature for 0.8PMN-0.2PT ceramics with decreasing grain sizes. Measurements on heating were carried out after maintaining the sample at 77 K for 1 h.

grain size of 0.14 μm are shown in Fig. 8(a), measured during heating from 77 K to RT with 3.5 kV mm^{-1} . Direct comparison of the electric displacement loops at different temperatures was difficult because of differences in permittivity. To this aim, loops were compensated for linear polarization and conduction contributions, which were determined from the current response under a low field of 0.2 kV mm^{-1} and

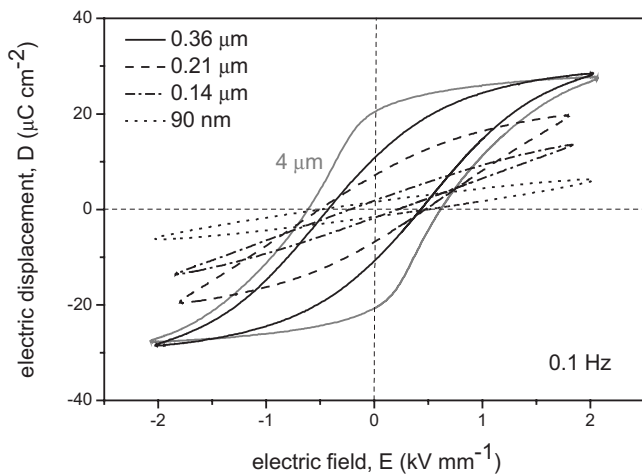


FIG. 7. Room-temperature ferroelectric hysteresis loops for 0.8PMN-0.2PT ceramics with decreasing grain sizes down to the nanoscale.

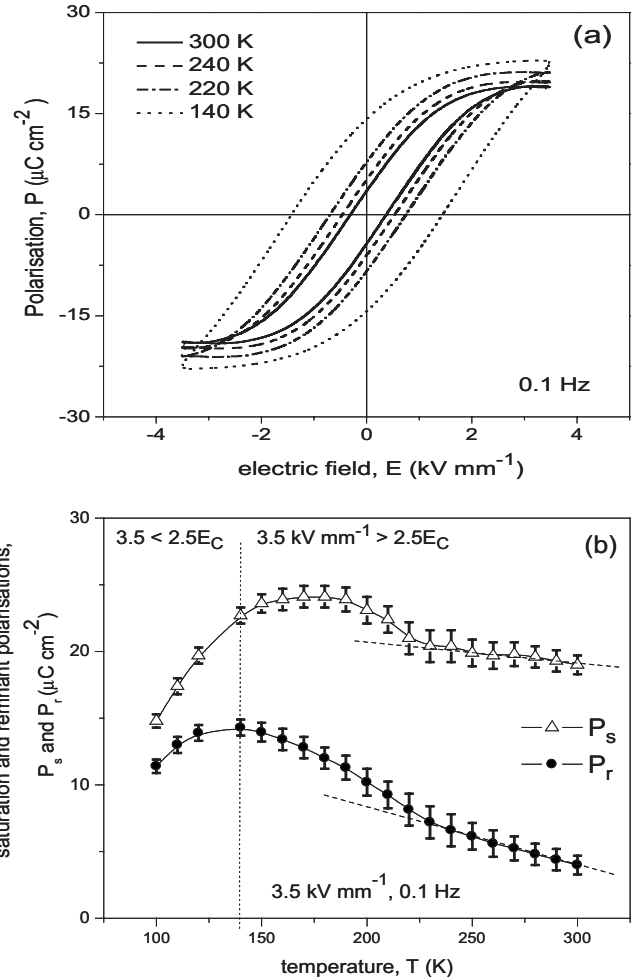


FIG. 8. (a) Ferroelectric hysteresis loops, and (b) saturation P_s and remnant P_r polarizations as a function of temperature for a 0.8PMN-0.2PT ceramic with an average grain size of $0.14 \mu\text{m}$. E_c stands for coercive field.

0.1 Hz. The sample was maintained at 77 K for 1 h before starting the measurement. Lack of saturation was initially observed with the highest field attainable in these experiments because of high coercive field E_c . This parameter continuously decreased as temperature increases, such as the maximum field exceeded $2.5E_c$ at 140 K, value from which saturation is usually assumed. Values for the saturation and remnant polarizations are given in Fig. 8(b). Maximum P_s and P_r of 23 and $14 \mu\text{C cm}^{-2}$, respectively, were achieved at 140 K that dropped down to 19 and $4 \mu\text{C cm}^{-2}$ at RT. Note the change of slope at 230 K, which is the same temperature at which a mechanical anomaly was observed.

IV. DISCUSSION

Results for the ceramic material with a grain size of $0.36 \mu\text{m}$ are basically the same as previously reported for a coarse-grained material as far as the dynamics of the relaxor and the transition between the ferroelectric and relaxor states are concerned. Equal freezing temperature and activation energy values are obtained from the fit of the data to the Vogel-

Fulcher relationship: 350 K and 30 meV,²⁸ which suggests that the dynamics of the relaxor state is not significantly modified when size is decreased down to 0.36 μm . Also very similar temperature dependences of permittivity and Young's modulus across the transition were found for the submicrostructured material, which indicates that the main features of the transition persist with a size of 0.36 μm . The transition is still between the monoclinic Cm ferroelectric phase, as determined by Rietveld analysis of XRD data,²⁷ and the nonergodic relaxor state with well defined, separated transition ($T_{Ch}=338$ K and $T_{Cc}=328$ K on heating and cooling, respectively) and freezing ($T_f=350$ K) temperatures. Therefore, the main effect of decreasing grain size from 4 down to 0.36 μm is the shift of the transition temperatures, from 344 and 334 K to 338 and 328 K. The thermal hysteresis in the kinetics, the transition is much slower on cooling than on heating in a coarse-grained ceramic, is also observed in the submicrostructured material. This hysteresis was associated with the existence of a well defined temperature of slowing down of the transition within the interval between the transition temperatures on cooling and heating. These are 334–344 K and 328–338 K for the coarse-grained and submicrostructured ceramics, respectively. If one assumes that the transition is slowed down at the same temperature in the two materials, it can be argued that the slowing down must take place between 334 and 338 K.

The parameters of the Vogel-Fulcher behavior of the high-temperature relaxor state for the ceramic materials with a grain size of 0.21 and 0.14 μm are also very similar to those of the ceramics with larger grain size. This indicates that the dynamics of the relaxor state is also not modified down to 0.14 μm . However, the thermal hysteresis observed around the phase transition, with a slow kinetics, disappears for the lowest transition temperatures. This occurs when the transition temperatures on heating are shifted down to 332 and 304 K for the materials with a grain size of 0.21 and 0.14 μm , respectively. This is consistent with the existence of a well defined temperature of slowing down of the transition in 0.8PMN-0.2PT within the interval 334–338 K, and provides further support to the two-stage model for the development of ferroelectric long-range order in relaxor systems.³⁰

In this model, in a first stage at high temperature, PNRs start condensing at the Burns' temperature,⁴² which is at 670 K for 0.8PMN-0.2PT.⁴³ Their number and size increase as the temperature is decreased until approaching the temperature of the phase transition.⁴⁴ Then, a second stage begins that is characterized by the onset of ferroelectric fluctuations. The model proposes that the kinetics of the transition is controlled by the number of PNRs at the onset of the ferroelectric fluctuations, which is highly dependant on the transition temperature. That is, the slower the kinetics the higher the number of PNRs, the lower the temperature of the transition. Results indicate that a quite sharp slowing down of the transition between the relaxor and ferroelectric states takes place within the interval 334–338 K for 0.8PMN-0.2PT. They also show that a size effect appears in its kinetics when the transition temperatures are shifted down out of this interval with the decrease in grain size below 0.36 μm .

However, not only the time scale of the transition is affected. According to the model of Ye *et al.*,³⁰ the kinetics

controls the final states. 0.7PMN-0.3PT presents transition temperatures ($T_{Ch}=402$ K and $T_{Cc}=408$ K) above the interval of temperatures at which the slowing down occurs, therefore the kinetics of the transition is fast³⁷ and a well developed ferroelectric monoclinic Cm long-range order results.³¹ When transition temperatures are below the temperature of slowing down, such as for 0.9PMN-0.1PT,⁴⁴ the kinetics is slow and a rhombohedral $R3m$ order results, yet a monoclinic local order exists that is evidenced by the observation of short-range shifts of the Pb^{2+} cations along the $\langle 110 \rangle$ directions in addition to the $\langle 111 \rangle$ long-range rhombohedral shift.⁴⁴ For PMN, the transition would be extremely slow, and whether a ferroelectric state is developed is under debate.^{45–47} Note that we found a similar evolution with the variation of grain size (see Table I), which is also associated with the slowing down of the kinetics of the transition. 0.8PMN-0.2PT ceramics with grain sizes of 0.21 μm or larger present the transition temperatures above or close to the temperature of slowing down and a monoclinic phase at RT. Ceramics with grain sizes of 0.14 μm and smaller present the rhombohedral phase, typical of slow kinetics of the transition. This indicates that the kinetics controls the scale of the monoclinic order, i.e., the size of the monoclinic domains. This size in turn usually affects domains own dynamics and thus, polarization switching. As a matter of fact, the ferroelectric hysteresis loops of coarse-grained 0.8PMN-0.2PT ceramics are leant as compared with those for 0.7PMN-0.3PT ceramics with the same grain size, both compositions monoclinic Cm , which has been associated with differences in the domain size arising from the slower kinetics of the transition for 0.8PMN-0.2PT.²⁸ Leant loops have been observed for 0.75PMN-0.25PT single crystals along the $\langle 110 \rangle$ direction and also associated with a speckled domain configuration with sizes ranging from 8 μm^2 to less than 100 nm^2 .⁴⁸ Therefore, the evolution of the ferroelectric hysteresis loops for the 0.8PMN-0.2PT ceramics with grain size at RT, shown in Fig. 7, can be understood as a consequence of the change of the scale in the monoclinic order; the saturation and remnant polarizations decrease with grain size, so as only incipient switching is observed for ceramics with grains smaller than 0.21 μm with an applied field of 2 kV mm^{-1} (a field high enough to saturate the loops for coarse-grained materials). This is the grain size below which an average rhombohedral phase is indicated by the Rietveld analysis. The polarizations of these very fine grained ceramics increase when the field is increased, up to $P_s=19$ and $P_r=4$ $\mu\text{C cm}^{-2}$ with 3.5 kV mm^{-1} for the ceramic with a grain size of 0.14 μm , and by cooling below RT (see Fig. 8), which is most probably a consequence of the coarsening of the monoclinic domains under high field or on decreasing temperature.

This was confirmed by Rietveld analysis of the XRD pattern of the ceramic with the grain size of 0.14 μm at 100 K. Procedures and methodology were the same as used in previous studies on the PMN-PT samples.^{27,28} Results are given in Table III along with those at 295 K and show that the average symmetry changes from rhombohedral $R3m$ to monoclinic Cm on cooling, as proposed.

Finally, results also indicate that the dynamics of the high-temperature relaxor state are modified at the nanoscale, with

TABLE III. Agreement factors of the Rietveld analysis of XRD data for a 0.8PMN-0.2PT ceramic with a grain size of 0.14 μm at 295 and 100 K. Results for $R3m$ and Cm symmetries are shown, which consistently gave the best agreements among the models tested. Cell parameters for the phase with the lowest factors are also included.

Temperature	Symmetry					
	$R3m$		Cm			
	R_{wp}	GoF	R_{Bragg}	R_{wp}	GoF	R_{Bragg}
295 K	7.07	1.35	2.57	7.15	1.36	2.97
			$a=4.0300 \text{ \AA}, \beta=89.99^\circ$			
100 K	8.50	1.45	4.72	8.38	1.43	3.52
			$a=5.6949 \text{ \AA}, b=5.6880 \text{ \AA}, c=4.0287 \text{ \AA}, \beta=89.92^\circ$			

a decrease of the freezing temperature down to 340 K and an increase of the activation energy up to 47 meV when the grain size is reduced down to 90 nm. A size effect might be expected when the grain size approaches the characteristic size of the polar nanoregions. This size has been shown to be ~ 10 nm for PMN at 5 K (Ref. 49) and decreases when the temperature is increased.⁴⁴ However, the smallest grain size here investigated is still an order of magnitude higher than the size of the PNRs, and a significant modification of the interactions among them (random bonds) is thus not expected. Also, a perturbation of the relaxor state has been proposed to occur for PMN at an outer shell associated with the grain boundary, which would present a smaller polarizability than the bulk.⁵⁰ The modification of the Vogel-Fulcher parameters in nanostructured 0.8PMN-0.2PT could just reflect a different dynamics of the relaxor at the shell, which might be also responsible for the decrease of the maximum permittivity of the ceramic samples when grain size decreases.

Mechanisms behind size effects in 0.8PMN-0.2PT might be generally valid for relaxor-based systems. For instance, an evolution from monoclinic Pm micron-sized lamellar domains to submicron/nanometer sized crosshatched domains has been recently described for 0.65PMN-0.35PT ceramics when grain size is reduced from 4 to 0.15 μm , which is accompanied with relaxor-type electrical behavior and hindered ferroelectric switching.⁵¹ These size effects are qualitatively analogous to those here described and could also originate from the shift of the transition temperatures below that of slowing down of its kinetics in the submicron range, which would be thus a characteristic of relaxor-based systems. Also, slowing down of the transition has been reported for 0.955PZN-0.045PT single crystals.⁵²

One last issue worth discussing is the origin of the elastic anomaly at ~ 235 K, which is also the temperature below which the saturation and remnant polarizations of the hysteresis loops significantly increase. The peak in mechanical losses at ~ 235 K is coupled with that associated with the ferroelectric transition; one increases when the other decreases, which suggests the low-temperature anomaly to be caused by some volume of the material undergoing the transition at 235 K. The size effect, the height of the low-temperature peak in mechanical losses increases as the size decreases, indicates that it is most probably a skin effect.

Thus, there is an outer shell next to the grain boundary that does not transform into the ferroelectric phase until 235 K, which is consistent with the enhancement of ferroelectric switching below this temperature. This phenomenon might be associated with the perturbation of the relaxor state next to the grain boundary previously discussed, yet its origin is not known.

V. SUMMARY AND CONCLUSIONS

The results here presented shed light onto the origin of the size effects on the room-temperature phases and ferroelectric behavior of 0.8PMN-0.2PT. They are related to the observed decrease of the transition temperature with grain size, which results in a slowing down of its kinetics below a certain value ($g=0.36 \mu\text{m}$). In agreement with the two-stage model for the development of ferroelectric long-range order in relaxor systems,^{28–30} this result implies that a temperature of slowing down of the transition must be well defined. For the system 0.8PMN-0.2PT it is within the interval of 334–338 K, according to our results. But the study of the behavior of these ceramics also allows us to conclude that the scale of the Cm monoclinic distortions within the average $R3m$ rhombohedral phase, whose evolution with the content of PbTiO_3 in this solid solution has extensively been studied, may be mostly controlled by the kinetics of the transition, and, therefore, influenced by grain size. In fact, it decreases when grain size decreases and increases when temperature is lowered. In turn, it has been shown that the scale of the monoclinic order strongly influences their ferroelectric behavior as switching is hindered by its shrinkage. This is most probably correlated with an evolution of the domain configuration with grain size, which will be the subject of further work. Additionally, results also suggest the presence of a shell next to the grain boundary, at which the relaxor state is perturbed, and stabilized down to ferroelectric state at lower temperature than the core.

ACKNOWLEDGMENTS

This research has been funded by MEC through Project No. MAT2005-01304. Collaboration between ICMM and IJS is framed within the EC NoE MIND (Contract No. NoE 515757-2). H.A. also acknowledges support by MEC through the JdC Programme.

- ¹ *Piezoelectric Materials in Devices*, edited by N. Setter (EPFL, Lausanne, Switzerland, 2002).
- ² B. Noheda, J. A. Gonzalo, L. E. Cross, R. Guo, S.-E. Park, D. E. Cox, and G. Shirane, *Phys. Rev. B* **61**, 8687 (2000).
- ³ R. Guo, L. E. Cross, S. E. Park, B. Noheda, D. E. Cox, and G. Shirane, *Phys. Rev. Lett.* **84**, 5423 (2000).
- ⁴ H. Fu and R. E. Cohen, *Nature (London)* **403**, 281 (2000).
- ⁵ T. Takahashi, *Ferroelectrics* **41**, 143 (1982).
- ⁶ B. Noheda, D. E. Cox, G. Shirane, S. E. Park, L. E. Cross, and Z. Zhong, *Phys. Rev. Lett.* **86**, 3891 (2001).
- ⁷ A. K. Singh, D. Pandey, and O. Zaharko, *Phys. Rev. B* **74**, 024101 (2006).
- ⁸ R. Haumont, B. Dkhil, J. M. Kiat, A. Al-Barakaty, H. Dammak, and L. Bellaiche, *Phys. Rev. B* **68**, 014114 (2003).
- ⁹ S. E. Park and T. R. Shrout, *J. Appl. Phys.* **82**, 1804 (1997).
- ¹⁰ S. Kwon, E. M. Sabolsky, G. L. Messing, and S. Trolier-McKinstry, *J. Am. Ceram. Soc.* **88**, 312 (2005).
- ¹¹ C. Pithan, D. Hennings, and R. Waser, *Int. J. Appl. Ceram. Technol.* **2**, 1 (2005).
- ¹² K. Uchino, *Acta Mater.* **46**, 3745 (1998).
- ¹³ S. Trolier-McKinstry and P. Muralt, *J. Electroceram.* **12**, 7 (2004).
- ¹⁴ G. Arlt, D. Hennings, and G. Dewith, *J. Appl. Phys.* **58**, 1619 (1985).
- ¹⁵ G. Arlt, *Ferroelectrics* **104**, 217 (1990).
- ¹⁶ T. Hungría, T. M. Algueró, A. B. Hungría, and A. Castro, *Chem. Mater.* **17**, 6205 (2005).
- ¹⁷ G. Arlt, *J. Mater. Sci.* **25**, 2655 (1990).
- ¹⁸ M. Demartin and D. Damjanovic, *Appl. Phys. Lett.* **68**, 3046 (1996).
- ¹⁹ A. G. Zembilgotov, N. A. Pertsev, and R. Waser, *J. Appl. Phys.* **97**, 114315 (2005).
- ²⁰ S. Tsunekawa, S. Ito, T. Mori, K. Ishikawa, Z. Q. Li, and Y. Kawazoe, *Phys. Rev. B* **62**, 3065 (2000).
- ²¹ C. H. Ahn, K. M. Rabe, and J. M. Triscone, *Science* **303**, 488 (2004).
- ²² X. Deng, X. Wang, H. Wen, L. Chen, L. Chen, and L. Li, *Appl. Phys. Lett.* **88**, 252905 (2006).
- ²³ C. A. Randall, N. Kim, J. P. Kucera, W. Cao, and T. R. Shrout, *J. Am. Ceram. Soc.* **81**, 677 (1998).
- ²⁴ K. S. Seol and K. Takeuchi, *Appl. Phys. Lett.* **85**, 2325 (2004).
- ²⁵ J. Carreaud, P. Geimeiner, J. M. Kiat, B. Dkhil, C. Bogicevic, T. Rojac, and B. Malic, *Phys. Rev. B* **72**, 174115 (2005).
- ²⁶ M. Algueró, T. Hungría, H. Amorín, J. Ricote, J. Galy, and A. Castro, *Small* **3**, 1906 (2007).
- ²⁷ J. Carreaud, J. M. Kiat, B. Dkhil, M. Algueró, J. Ricote, R. Jiménez, J. Holc, and M. Kosec, *Appl. Phys. Lett.* **89**, 252906 (2006).
- ²⁸ R. Jiménez, B. Jiménez, J. Carreaud, J. M. Kiat, B. Dkhil, J. Holc, M. Kosec, and M. Algueró, *Phys. Rev. B* **74**, 184106 (2006).
- ²⁹ A. A. Bokov, *Phys. Solid State* **36**, 19 (1994).
- ³⁰ Z. G. Ye, Y. Bing, J. Gao, A. A. Bokov, P. Stephens, B. Noheda, and G. Shirane, *Phys. Rev. B* **67**, 104104 (2003).
- ³¹ A. K. Singh and D. Pandey, *Phys. Rev. B* **67**, 064102 (2003).
- ³² D. Kuscer, J. Holc, and M. Kosec, *J. Am. Ceram. Soc.* **90**, 29 (2007).
- ³³ M. Algueró, A. Moure, L. Pardo, J. Holc, and M. Kosec, *Acta Mater.* **54**, 501 (2006).
- ³⁴ M. Algueró, C. Alemany, B. Jiménez, J. Holc, M. Kosec, and L. Pardo, *J. Eur. Ceram. Soc.* **24**, 937 (2004).
- ³⁵ H. Amorin, J. Ricote, R. Jiménez, J. Holc, M. Kosec, and M. Algueró, *Scr. Mater.* **58**, 755 (2008).
- ³⁶ R. Jiménez, A. Castro, and B. Jiménez, *Appl. Phys. Lett.* **83**, 3350 (2003).
- ³⁷ M. Algueró, B. Jiménez, and L. Pardo, *Appl. Phys. Lett.* **87**, 082910 (2005).
- ³⁸ M. Algueró, B. Jiménez, and L. Pardo, *Appl. Phys. Lett.* **83**, 2641 (2003).
- ³⁹ M. T. Buscaglia, M. Viviani, V. Buscaglia, L. Mitoseriu, A. Testino, P. Nanni, Z. Zhao, M. Nygren, C. Harnagea, D. Piazza, and C. Galassi, *Phys. Rev. B* **73**, 064114 (2006).
- ⁴⁰ B. Jiménez and R. Jiménez, *Phys. Rev. B* **66**, 014104 (2002).
- ⁴¹ A. V. Kityk, W. Schranz, P. Sondergeld, D. Havlik, E. K. H. Salje, and J. F. Scott, *Phys. Rev. B* **61**, 946 (2000).
- ⁴² G. Burns and F. H. Dacol, *Phys. Rev. B* **28**, 2527 (1983).
- ⁴³ T. Y. Koo, P. M. Gehring, G. Shirane, V. Kiryukhin, S. G. Lee, and S. W. Cheong, *Phys. Rev. B* **65**, 144113 (2002).
- ⁴⁴ B. Dkhil, J. M. Kiat, G. Calvarin, G. Baldinozzi, S. B. Vakhru-shev, and E. Suard, *Phys. Rev. B* **65**, 024104 (2001).
- ⁴⁵ S. Wakimoto, C. Stock, R. J. Birgeneau, Z. G. Ye, W. Chen, W. J. L. Buyers, P. M. Gehring, and G. Shirane, *Phys. Rev. B* **65**, 172105 (2002).
- ⁴⁶ S. Kamba, M. Kempa, V. Bovtun, J. Petzelt, K. Brinkman, and N. Setter, *J. Phys.: Condens. Matter* **17**, 3965 (2005).
- ⁴⁷ E. V. Colla, M. B. Weissman, P. M. Gehring, G. Xu, H. Luo, P. Gemeiner, and B. Dkhil, *Phys. Rev. B* **75**, 024103 (2007).
- ⁴⁸ X. Zhao, J. Y. Dai, J. Wang, H. L. W. Chan, C. L. Choy, X. M. Wan, and H. S. Luo, *Phys. Rev. B* **72**, 064114 (2005).
- ⁴⁹ N. de Mathan, E. Husson, G. Calvarin, J. R. Gavarrí, A. W. Hewat, and A. Morrell, *J. Phys.: Condens. Matter* **3**, 8159 (1991).
- ⁵⁰ P. Papet, J. P. Dougherty, and T. R. Shrout, *J. Mater. Res.* **5**, 2902 (1990).
- ⁵¹ M. Algueró, J. Ricote, R. Jiménez, P. Ramos, J. Carreaud, B. Dkhil, J. M. Kiat, J. Holc, and M. Kosec, *Appl. Phys. Lett.* **91**, 112905 (2007).
- ⁵² J. H. Ko, D. H. Kim, S. Kojima, W. Z. Chen, and Z. G. Ye, *J. Appl. Phys.* **100**, 066106 (2006).